Journal of Inflammation Research Dovepress

Open Access Full Text Article ORIGINAL RESEARCH

Decreasing of Trimethylamine N-Oxide by Cecal Microbiota and Choline-Trimethylamine Lyase are Associated with Sishen Pill on Diarrhea with Kidney-Yang Deficiency Syndrome

Mingmin Guo[1,2], Yi Wu[2,3], Maijiao Peng[1,2], Nenqun Xiao[1,2], Zhijun Lei[1,2], Zhoujin Tan[2,3]

[1]School of Pharmacy, Hunan University of Chinese Medicine, Changsha, People's Republic of China; [2]Hunan Key Laboratory of Traditional Chinese Medicine Prescription and Syndromes Translational Medicine, Changsha, People's Republic of China; [3]School of Traditional Chinese Medicine, Hunan University of Chinese Medicine, Changsha, People's Republic of China

Correspondence: Zhijun Lei, School of Pharmacy, Hunan University of Chinese Medicine, Changsha, 410208, People's Republic of China, Email lzj-707@163.com; Zhoujin Tan, School of Traditional Chinese Medicine, Hunan University of Chinese Medicine, Changsha, 410208, People's Republic of China, Email tanzhjin@sohu.com

Background: Sishen Pill (SSP) is a traditional Chinese medicine prescription commonly used to treat diarrhea with kidney-yang deficiency syndrome. The aim was to investigate the underlying mechanisms of SSP's therapeutic effects, providing experimental evidence for its mechanism of action.

Methods: A mouse model of diarrhea with kidney-yang deficiency syndrome was induced using adenine combined with *Folium sennae*. After successful model replication, SSP decoction was administered. CutC activity, TMAO, IL-6, TNF-α levels, and cecal content microbiota were measured.

Results: SSP significantly improved the general behavioral characteristics of diarrhea mice, and reduced CutC activity, TMAO and IL-6 levels. Sequencing results indicated significant changes at the phylum and genus levels. Correlation analysis revealed a positive correlation between CutC activity and *Faecalibaculum* ($p<0.05$) and *Chryseobacterium* ($p<0.05$), and a significant negative correlation with *Prevotellaceae UCG−001, Rikenella* ($p<0.05$), *Acinetobacter* ($p<0.05$), *Parasutterella* ($p<0.05$), and *Lacticaseibacillus* ($p<0.05$). TNF-α levels showed a significant negative correlation with *Lacticaseibacillus* ($p<0.05$), *Prevotellaceae UCG−001* ($p<0.01$), *Parasutterella* ($p<0.05$), and *Candidatus Saccharimonas* ($p<0.05$). IL-6 levels exhibited a significant negative correlation with *Rikenella* ($p<0.05$), *Acinetobacter* ($p<0.05$), *Prevotellaceae UCG−001* ($p<0.05$), *Lacticaseibacillus* ($p<0.01$), and *Parasutterella* ($p<0.05$), and a significant positive correlation with *Faecalibaculum* ($p<0.05$), *Chryseobacterium* ($p<0.01$), and *A2*. Serum TMAO levels showed a significant positive correlation with *Faecalibaculum* ($p<0.05$) and *Chryseobacterium* ($p<0.01$), and hepatic TMAO levels exhibited a significant positive correlation with *Chryseobacterium* ($p<0.05$).

Conclusion: SSP significantly alleviated the symptoms of diarrhea with kidney-yang deficiency syndrome by modulating the cecal microbiota, downregulating CutC activity, and reducing TMAO and inflammatory factor levels. The cecal microbiota-CutC-TMAO-inflammatory cytokine axis may be a key mechanism underlying the therapeutic effects of SSP.

Keywords: Diarrhea, Kidney-Yang Deficiency Syndrome, Sishen Pill, CutC, Cecal microbiota, TMAO, Inflammation

Introduction

Diarrhea is defined as having more than 3 bowel movements per day, increased water content in stools, and loose or watery stool consistency. It is a common global public health issue that significantly impacts the physical and mental health as well as the quality of life of affected individuals.[1] The earliest discussions on diarrhea in traditional Chinese medicine (TCM) can be found in the "Huang Di Nei Jing" ("Yellow Emperor's Inner Canon"). Due to variations in the etiology, pathogenesis, and clinical manifestations of diarrhea, different TCM patterns are observed, with kidney-yang deficiency syndrome being one of the common patterns associated with diarrhea.[2] The hallmark of diarrhea with kidney-yang deficiency syndrome is its

Received: 24 June 2024
Accepted: 27 September 2024
Published: 13 October 2024

© 2024 Guo et al. This work is published and licensed by Dove Medical Press Limited. The full terms of this license are available at https://www.dovepress.com/terms.php and incorporate the Creative Commons Attribution – Non Commercial (unported, v3.0) License (http://creativecommons.org/licenses/by-nc/3.0/). By accessing the work you hereby accept the Terms. Non-commercial uses of the work are permitted without any further permission from Dove Medical Press Limited, provided the work is properly attributed. For permission for commercial use of this work, please see paragraphs 4.2 and 5 of our Terms (https://www.dovepress.com/terms.php).

occurrence predominantly in the early morning, characterized by loose, watery stools, accompanied by a sensation of body coldness and icy cold limbs.[2,3] In previous studies, our research team successfully established a mouse model of diarrhea with kidney-yang deficiency syndrome using adenine combined with *Folium sennae*.[2,3] Adenine combined with *Folium sennae* administered via gavage is a well-established method to prepare a mouse model of diarrhea with kidney-yang deficiency syndrome. Adenine, under the action of xanthine oxidase, generates 2.8-dihydroxyadenine, which is insoluble in water and accumulates in the renal tubules and interstitium, causing renal function damage. This accumulation also impedes the metabolism of substances such as sugars, fats, and proteins, thereby affecting the body's energy metabolism and leading to the formation of kidney-yang deficiency syndrome. Following gastric lavage with *Folium sennae*, mice exhibit evident symptoms of diarrhea.[2,4]

The intestinal microbiota plays a crucial role in maintaining human health. Under normal conditions, it establishes a dynamic ecological balance between the host and the external environment. Disruption of this balance can lead to various host dysfunctions, such as loss of barrier function, inflammation, and immune dysfunction, which may trigger disease.[5–7] Diarrhea and intestinal microbiota disorder exhibit a bidirectional relationship: diarrhea frequently coexists with intestinal microbiota imbalance, and disruption of bacterial microbiota can subsequently exacerbate diarrhea. Compared to non-diarrheal individuals, those with diarrhea exhibit significant differences in the composition of their intestinal microbiota, showing a higher abundance of Bacteroides and a lower abundance of Firmicutes. Furthermore, microbiota dysbiosis can further exacerbate diarrhea.[3,8] In antibiotic-associated diarrhea mice, there is a decrease in intestinal microbiota diversity, and changes in intestinal microbiota abundance and composition lead to further dysfunction in microbiota function.[9] Previous studies have found that diarrhea with kidney-yang deficiency syndrome mice exhibit dysbiosis in the cecal microbiota, with a notable reduction in beneficial bacteria.[10] The imbalance in microbiota is a crucial factor in the occurrence of diarrhea with kidney-yang deficiency syndrome.

One of the main ways in which the intestinal microbiota interacts with the host is through metabolites. The intestinal microbiota can produce biologically active metabolites, directly or indirectly affecting the host's physiological functions. Disruption of the microbiota structure can reduce the production of beneficial metabolites and increase the accumulation of harmful metabolites. Trimethylamine N-oxide (TMAO) is one of the choline metabolites produced by the intestinal microbiota and is considered a gut-derived uremic toxin.[11] Choline, under the action of choline-trimethylamine lyase (CutC) produced by the intestinal microbiota, is converted to trimethylamine (TMA), the main source of TMA in the gut, primarily produced in the cecum. TMA is absorbed through the intestinal wall and reaches the liver via the portal vein, where it is rapidly oxidized to form TMAO catalyzed by flavin-containing monooxygenases (FMOs), mainly FMO3.[12,13] In the pathway of TMAO formation, two important enzymes are involved, and the activity of these enzymes can affect the levels of TMAO. Inhibiting FMO3 activity can reduce TMAO levels but may lead to TMA accumulation, resulting in the "fish odor syndrome". The strong activity of CutC enzyme produced by the intestinal microbiota is a focus of research to reduce the harmful metabolite TMAO.[13,14] Microbes that produce CutC are primarily found in the cecum. Anaerobic degradation of choline by CutC is considered the main source of TMA formation in the intestine, and TMA is mainly produced in the cecum. Therefore, the cecal microbiota is the optimal focus for this study.

TMAO can participate in the development of cardiovascular and chronic kidney diseases by activating p38 phosphorylation and upregulating human antigen HuR, thereby increasing the expression of inflammatory cytokines such as tumor necrosis factor-alpha (TNF-α) and interleukin-6 (IL-6).[13,14] Elevated levels of inflammatory cytokines are closely related to diarrhea. Increased expression of TNF-α and IL-6 enhances the permeability of vascular endothelial cells, leading to leakage of intestinal fluid and causing diarrhea.[15] Furthermore, elevated serum TNF-α levels in IBS-D patients exacerbate immune dysfunction of the intestinal mucosa, induce inflammatory responses, and promote disease recurrence. TMAO-induced release of inflammatory cytokines associated with diarrhea with kidney-yang deficiency syndrome is related to TNF-α and IL-6 levels. TMAO participates in the disease process by regulating inflammatory cytokine levels and may be associated with intestinal microbiota dysbiosis. The abnormal expression of a large number of inflammatory cytokines, once entering the bloodstream and circulating to the intestines, causes congestion and edema of the intestinal wall. Subsequent intestinal ischemia and hypoxia can disrupt the intestinal mucosal barrier, further causing microbial imbalance.

Sishen Pill is a classical formula for treating diarrhea with kidney-yang deficiency syndrome. SSP was first recorded in the "Chen's Treatise on Pediatric Smallpox and Measles". This formula consists of six ingredients: *Psoralea corylifolia* L., *Myristica fragrans* Houtt., *Evodia rutaecarpa* (Juss). Benth., *Schisandra chinensis* (Turcz). Baill., *Zingiber officinale* Rosc., and *Ziziphus jujuba* Mill. The composition ratio is 4:2:1:2:2:2, with a total mass of 39 g. It functions to warm the kidneys and spleen, strengthen the intestines, and stop diarrhea.[3] Studies have found that it achieves therapeutic effects through the synergistic action of various bioactive substances.[16] It is commonly used in modern medicine for the treatment of inflammatory bowel disease, chronic colitis, irritable bowel syndrome, functional diarrhea, chronic diarrhea, and refractory diarrhea, showing good efficacy.[17–19] TCM is characterized by multiple components, targets, and modes of action in disease prevention and treatment. The intestinal microbiota, as one of its main targets, is closely related to the effectiveness of TCM.[20] In previous research, our team found that SSP effectively improves diarrhea by regulating the disrupted intestinal mucosal microbiota in a mouse model of diarrhea with kidney-yang deficiency syndrome.[3] Furthermore, SSP can treat colitis by modulating the composition of the intestinal microbiota and downregulating the expression of inflammatory factors.[19] The study found that SSP can significantly reduce the levels of Proteobacteria and Mycoplasma in the intestines of IBS-D model rats. Proteobacteria is a large group of bacteria that includes many pathogenic species, and an increase in its abundance can lead to intestinal microbiota imbalance.[21]

Previous studies have demonstrated that mice with diarrhea with kidney- yang deficiency syndrome exhibit dysbiosis in the cecal microbiota, along with elevated levels of CutC activity, TMAO, and inflammatory factors.[10] Additionally, research has identified a link between intestinal microbiota imbalance and increased TMAO concentrations, where TMAO can activate inflammatory responses and cytokines, contributing to diarrhea with kidney-yang deficiency syndrome through the "gut-kidney axis".[22] Hence, we hypothesize that SSP may influence CutC activity and TMAO levels by modulating the composition of the cecal microbiota, and affecting the inflammatory response thereby mediating the treatment of diarrhea. This study employed adenine combined with *Folium sennae* to construct a diarrhea with kidney-yang deficiency syndrome in mice. Subsequently, SSP was administered to these mice, and the influence of the TCM formula SSP on the cecal microbiota, CutC activity, TMAO level, and inflammatory response in mice with diarrhea with kidney-yang deficiency syndrome was investigated to explore the mechanism of its therapeutic action.

Material and Methods

Animal and Feeding

To eliminate the influence of gender on the gut microbiota, only male mice were used in this study.[23] Thirty male KM mice of SPF-grade, weighing 18–22 g, 4 weeks old were purchased from Hunan Slack Jingda Experimental Animal Co, Ltd. (Changsha, China, License No: SCXK (Xiang) 2019–0004). They were housed in separate cages in the barrier environment of the Experimental Animal Center of Hunan University of Chinese Medicine (License No: SYXK (Xiang) 2019–0009) at a temperature of 23–25°C, relative humidity of 50%-70%, and a 12-hour light/dark cycle. Mice were provided with ad libitum access to food and water. The feed was supplied by the Experimental Animal Center of Hunan University of Chinese Medicine and produced by Jiangsu Medisan Biopharmaceutical Co., Ltd. The nutritional composition included moisture, crude protein, crude fiber, crude fat, crude ash, calcium, total phosphorus, lysine, methionine, and cysteine. The experiment was approved by the Animal Ethics and Welfare Committee of Hunan University of Chinese Medicine and was conducted in accordance with the Guidelines for Humane Endpoint Review of Animal Experiments. (Ethics Number: LL2023081010).

Drug and Preparation

Adenine (Changsha Yaer Biology Co., LTD, Changsha, China, EZ7890C450). *Folium sennae* (Anhui Pure Traditional Chinese Medicine Co., Ltd, 2008232). Preparation of adenine suspension: Prepare a suspension with sterile water at a dosage of 50 mg/(kg•d), prepare and use immediately, and avoid light. Preparation of *Folium sennae* decoction: Place *Folium sennae* in a beaker with an appropriate amount of water, discard the water after soaking for 30 minutes, add 5 times the weight of the medicinal herbs, heat in a 75 °C water bath for 30 minutes, filter and collect the filtrate. Then add

an appropriate amount of water to the residue, heat in a 75 °C water bath for 15 minutes, filter, and collect the filtrate. Combine the filtrates, rotary evaporate at 75 °C to a concentration of 1 g/mL and store at 4 °C for later use.[3,24]

Composition and Dosage of SSP: *Psoraleae fructus* 12 g (produced by Hunan Sanxiang Traditional Chinese Medicine Co., Ltd., batch number: 2023010602), *Myristica semen* 6 g (produced by Hunan Hengyue Traditional Chinese Medicine Co., Ltd., batch number: 23020923), *Euodiae fructus* 3 g (produced by Anhui Pure Traditional Chinese Medicine Co., Ltd., batch number: 2302283), *Schisandrae chinensis* 6 g (produced by the First Affiliated Hospital of Hunan University of Chinese Medicine, batch number: HQ23030603), *Jujubae fructus* 6 g (produced by Anhui Boyao Qiancao Traditional Chinese Medicine Pieces Co., Ltd., batch number: 2304156), *Zingiberis rhizome recens* 6 g.[2,3,24] Preparation of SSP decoction: Soak the herbs in water for 30 minutes, discard the water, add 5 times the amount of water to the herbs, boiled at 100°C for 30 minutes, filter the liquid. Add an appropriate amount of water to the residue, repeat the heating and filtering process, combine the two liquids, and concentrate to 0.29 g/mL. The SSP decoction is stored at 4 °C for later use.[2,3,24]

Animal Grouping and Treatment

The animal experimental procedure is illustrated in Figure 1. Thirty mice were adaptively fed with free access to water and maintenance feed for 3 days. They were then randomly divided into the normal control group (Healthy) with 10 mice and the model group (MM) with 20 mice. Mice in the MM group were administered an adenine suspension by gavage continuously for 14 days at a dose of 50 mg/(kg·d), 0.4 mL/mouse, once a day.[2] Starting on the 8th day after the administration of the adenine suspension, mice in the MM group were also administered *Folium sennae* decoction by gavage for 7 consecutive days at a dose of 10 mg/(kg·d), 0.4 mL/mouse, once a day.[2] During this period, the Healthy group was given sterile water with the same volume and frequency. After successful model establishment, the 20 mice in the MM group were randomly divided into the model control group (Control) and the SSP group, with 10 mice in each group. Mice in the SSP group were administered SSP decoction by gavage for 7 days at a dose of 5 g/(kg·d), 0.35 mL/mouse, twice a day. The Healthy and Control groups were administered sterile water with the same volume and frequency.[3]

Animal Behavioral Observation

Using Healthy and Control group mice as controls, observe the mental status, spontaneous activity, fecal form and color, and perianal cleanliness of mice before and after SSP treatment. Record the daily average food and water intake of mice in each group during the treatment. On days 1, 3, and 7 of treatment, weigh and record the body weight and rectal temperature of the mice. Collect mouse feces at 9 a.m. on days 1, 3, and 7 of treatment, calculate the fecal water content, weigh and record the wet weight of the fecal sample, dry the sample at 110°C to constant weight, and record the dry weight.[25]

Model Evaluation Criteria

Based on the clinical manifestations of diarrhea with kidney-yang deficiency syndrome, the diagnostic criteria for macroscopic signs in the mouse model include loose stools or undigested grains in the feces, cold extremities, decreased

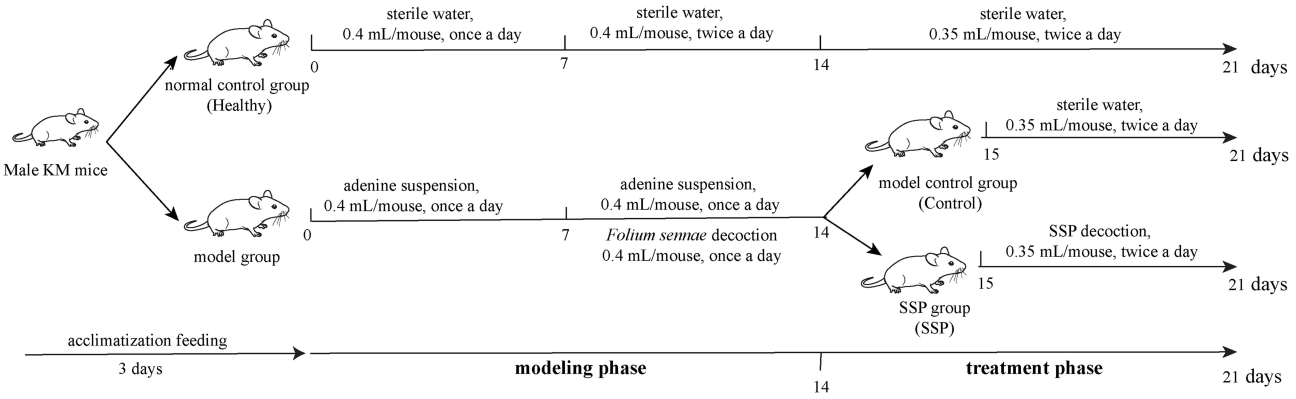

Figure 1 Flow chart of animal experiment. The administration method for all groups was via gavage.

appetite, and body weight, and a lethargic demeanor.[2,3] The collected feces were crushed and examined for the presence of loose stools or undigested particles to assess diarrhea based on fecal water content. Rectal temperature was used to evaluate limb coldness, while daily average food intake, daily average water intake, and body weight were used to assess reduced appetite and weight loss. The mental state of the mice was evaluated by observing squinting and clustering behavior.[2]

Sample Collection

After the treatment, mice were anesthetized with isoflurane inhalation, and blood was collected by enucleating the eyeball of mice. Blood samples collected from each group were allowed to stand at room temperature for 30 minutes, followed by centrifugation at 3000 rpm for 10 minutes. The upper layer of serum was then collected and transferred into Eppendorf tubes, which were stored at −80°C for subsequent ELISA assays. After cervical dislocation, the liver tissues of each mouse were collected and stored at −80 °C for later use in ELISA analysis. Under sterile conditions, sterile forceps were used to collect intestinal contents for CutC activity. Subsequently, the entire intestine was cut open with surgical scissors, and the intestinal mucosa was scraped after rinsing with physiological saline for the measurement of CutC activity. For each group, cecal contents and mucosa were collected from 5 mice for CutC activity measurement. Additionally, cecal contents from another set of 5 mice in each group were collected, labeled, and stored at −80 °C for subsequent 16S rRNA high-throughput sequencing.[3,26]

Measurement of CutC Activity

The small intestine contents and mucosa, the cecum contents and mucosa collected from each group were placed in sterilized conical bottles containing distilled water and glass beads, shaken for 30 minutes to extract the enzyme proteins fully, and then centrifuged at 3000 r/min for 15 minutes to collect the supernatant, which was used to prepare the crude enzyme solution. CutC activity was determined at a wavelength of 410nm using the picric acid–toluene method. This method is based on the catalysis of choline to TMA by CutC. The reaction of TMA with picric acid produces a yellow picric acid trimethylamine salt, which has an absorbance peak at 410nm. Therefore, the absorbance of the solution at 410nm was measured, and TMA was quantitatively analyzed using the standard curve method to calculate the activity of CutC.[27,28]

Enzyme-Linked Immunosorbent Assay

ELISA was used to detect the levels of IL-6, TNF-α, and TMAO in the serum and TMAO in liver. Blood samples collected from each group were allowed to stand at room temperature for 30 minutes, centrifuged at 3000r/min for 10 minutes, and the upper serum was transferred to ep tubes. The samples were then processed following the instructions of the kit, including adding samples, adding enzymes, incubation, plate washing, color development, stopping the reaction, and machine detection. Liver samples collected from each group were ground using a tissue grinder to obtain the supernatant, which was processed following the kit instructions for sample addition, enzyme addition, incubation, plate washing, color development, stopping the reaction, and machine detection. The IL-6, TNF-α, and TMAO kits were provided by Quanzhou Kenuodi Biotechnology Co., Ltd.

DNA Extraction, 16S rRNA Gene Amplicon Sequencing, and Sequence Analysis

(1) DNA Extraction: Total genomic DNA samples were extracted from cecal contents using the bacterial DNA extraction kit (produced by MP Biomedicals, batch number: 116564384). The quantity and quality of the extracted DNA were measured using a NanoDrop NC2000 spectrophotometer (Thermo Fisher Scientific, Waltham, MA, USA) and agarose gel electrophoresis, respectively.

(2) PCR Amplification: PCR amplification was performed using specific primers targeting the V3+V4 region of bacterial 16S rRNA. The forward primer sequence 338F (5′-ACTCCTACGGGAGGCAGCA-3′) and the reverse primer sequence 806R (5′-GGACTACHVGGGTWTCTAAT-3′) were used.

(3) PCR Product Recovery and Purification: PCR products were detected using 2% agarose gel electrophoresis, and purification was carried out using the Axygen® AxyPrep DNA Gel Extraction Kit.

(4) Fluorescent Quantification of PCR Products: The Quant-it PicoGreen dsDNA Assay Kit was used to quantitate the recovered PCR amplification products. Samples were mixed in proportion according to the sequencing volume requirements for each sample.
(5) Sequencing: Library construction was performed using the Illumina TruSeq Nano DNA LT Library Prep Kit, and sequencing was conducted using the Illumina NovaSeq 6000 platform with the NovaSeq 6000 SP Reagent Kit v1.5 (500 cycles) (Illumina, San Diego, CA, USA) in a 2*250bp sequencing mode. Sequencing was conducted by Shanghai Personal Biotechnology Co., Ltd. The sequencing data of the cecal content microbiota have been deposited in the NCBI database under the accession number: PRJNA1073021.

Bioinformatics Analysis

(1) Species annotation: Sequences were denoised to obtain ASVs according to the QIIME2 dada2 analysis workflow. The Silva database (http://www.arb-silva.de/) was selected, and the classify-sklearn algorithm from QIIME2 (https://github.com/QIIME2/q2-feature-classifier) was used for species annotation of each ASV feature sequence, using default parameters in QIIME2 and a pre-trained Naive Bayes classifier.
(2) Alpha diversity: Using the unrarefied ASV/OTU table, the "qiime diversity alpha-rarefaction" command is executed with parameters set to "–p-steps 10 –p-min-depth 10 –p-iterations 10", where the minimum rarefaction depth is set to 10. The parameter "–p-max-depth" is set to 95% of the sequencing depth of the sample with the lowest sequencing depth among all samples. Ten depth values are evenly selected between this depth and the minimum depth, and each depth value is rarefied 10 times to compute the chosen alpha diversity indices. The average score at the maximum rarefaction depth is used as the alpha diversity index.
(3) Rarefaction curve: The alpha-rarefaction.qzv file is generated by the "qiime diversity alpha-rarefaction" command. This file can be visualized by dragging it into https://view.qiime2.org/.[25]
(4) Beta diversity: Using the rarefied ASV table, the "qiime diversity core-metrics-phylogenetic" command is used to compute four distance matrices: Jaccard, Bray-Curtis, unweighted UniFrac, and weighted UniFrac. These distance matrices are then analyzed using PCoA, and a QZV file is outputted. The QZV file can be visualized by dragging it into the appropriate area on https://view.qiime2.org/.[29]
(5) Feature Microbiota Analysis: LEfSe (LDA Effect Size) analysis is a method that combines non-parametric Kruskal–Wallis and Wilcoxon rank-sum tests with Linear Discriminant Analysis (LDA) effect size. LEfSe analysis allows for simultaneous differential analysis at all taxonomic levels and emphasizes identifying robust differential taxa between groups, known as biomarker taxa. Using the unrarefied ASV table, the "classify_samples_ncv" function from q2-sample-classifier was called for random forest analysis.[30]
(6) Functional Prediction Analysis: Functional prediction of 16S rRNA sequence data was performed using PICRUSt2 2.3.0 based on the KEGG database.
(7) Correlation Analysis: Spearman analysis was conducted using the R stats package to explore the correlation between cecal content microbiota and CutC activity, TMAO levels, and inflammatory factors.

Statistical Analysis

Statistical processing and analysis were performed using SPSS 22.0 software. For metric data conforming to a normal distribution, the mean ± standard deviation was used to represent the data. When comparing two groups with samples that followed a normal distribution, *t*-test analysis was employed. If the distribution was non-normal, the Mann–Whitney *U*-test was used. For comparisons involving more than two groups, if the sample distribution was normal and the variances were homogenous, one-way analysis of variance (ANOVA) was applied, followed by LSD post hoc tests for further comparisons. If the data did not meet the assumptions of normal distribution or homogeneity of variance, the Kruskal–Wallis test was used. Count data from each group were expressed as percentages (%), and group comparisons were conducted using the chi-square test. The significance level was set at $\alpha=0.05$, and $p<0.05$ indicated statistical significance.

Results

Effects of SSP on General Behavior in Diarrhea with Kidney-Yang Deficiency Syndrome Mice

Mice in the Healthy group exhibited normal mental state and spontaneous activity, with dry bedding, well-formed stools, moderate softness, and cleanliness around the anus. Compared to the Healthy group, mice in the Control group showed poor mental state, reduced spontaneous activity, a tendency to gather in clusters, damp bedding, loose and sticky stools, and soiled perianal area. Mice in the SSP group showed some improvement in mental state, increased activity, and a reduction in clustering behavior (Figure 2). This indicates that the decoction of SSP can improve the symptoms and signs of mice with diarrhea with kidney-yang deficiency syndrome.

Throughout the experiment, the daily average food intake of the three groups of mice remained relatively stable (Figure 3A). With SSP intervention on days 1, 2, and 3, the food intake fluctuated significantly among the three groups. As the intervention time with SSP increased, the daily average food intake of the three groups tended to stabilize uniformly. From Figure 3B, it can be observed that, throughout the entire experimental process, the daily water intake of the Healthy group mice showed minimal fluctuations. The daily average water intake of Control group and SSP group mice was higher than that of the Healthy group. Starting from the SSP intervention, the daily average water intake of the

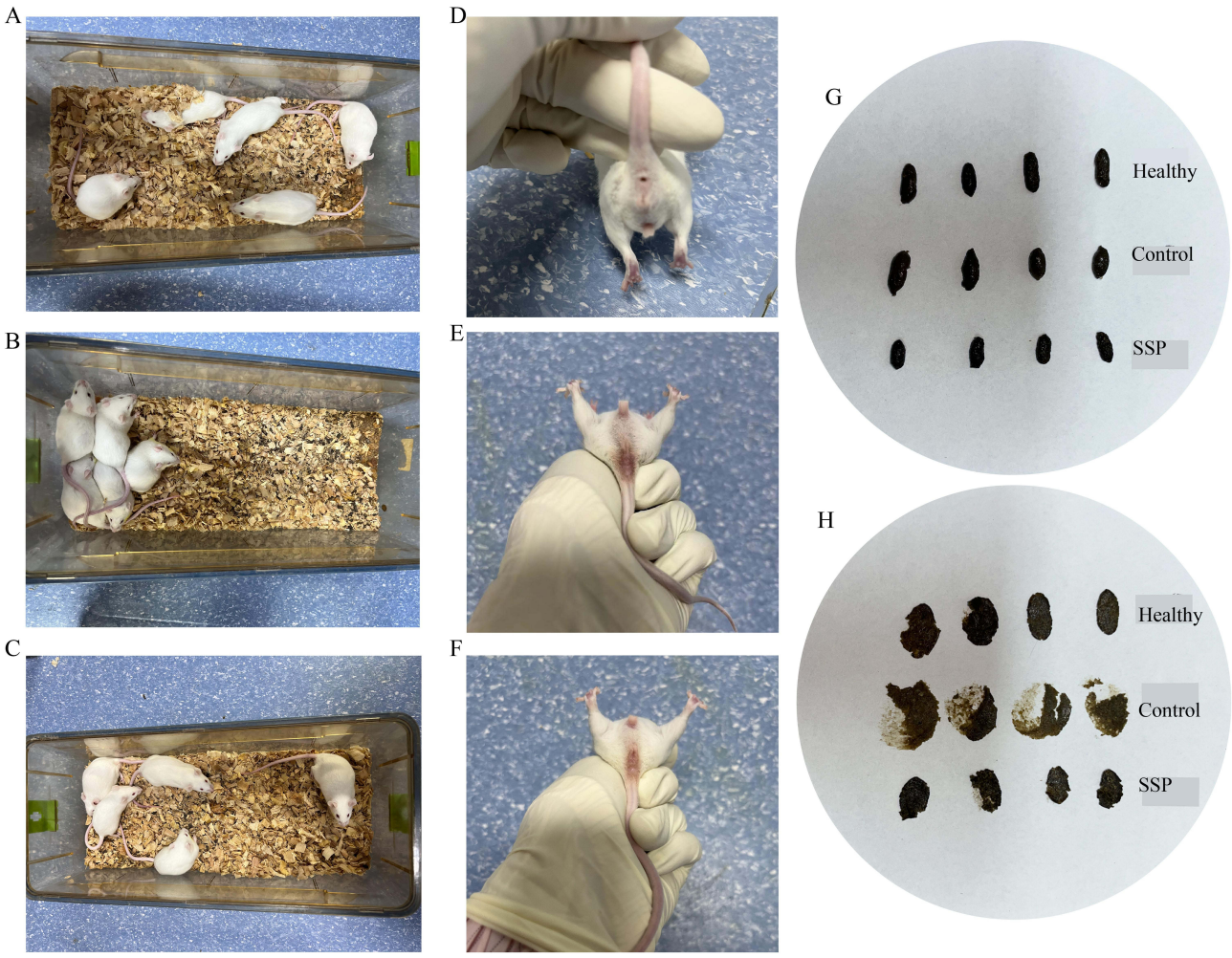

Figure 2 Effects of SSP on General Behavior in Diarrhea with Kidney-Yang Deficiency Syndrome Mice. (**A**) Behavioral and activity status of mice in the Healthy group; (**B**) Behavioral and activity status of mice in the Control group; (**C**) Behavioral and activity status of mice in the SSP group; (**D**) Perianal conditions of mice in the Healthy group; (**E**) Perianal conditions of mice in the Control group; (**F**) Perianal conditions of mice in the SSP group; (**G** and **H**) Fecal characteristics of the three groups of mice at the end of the experiment.

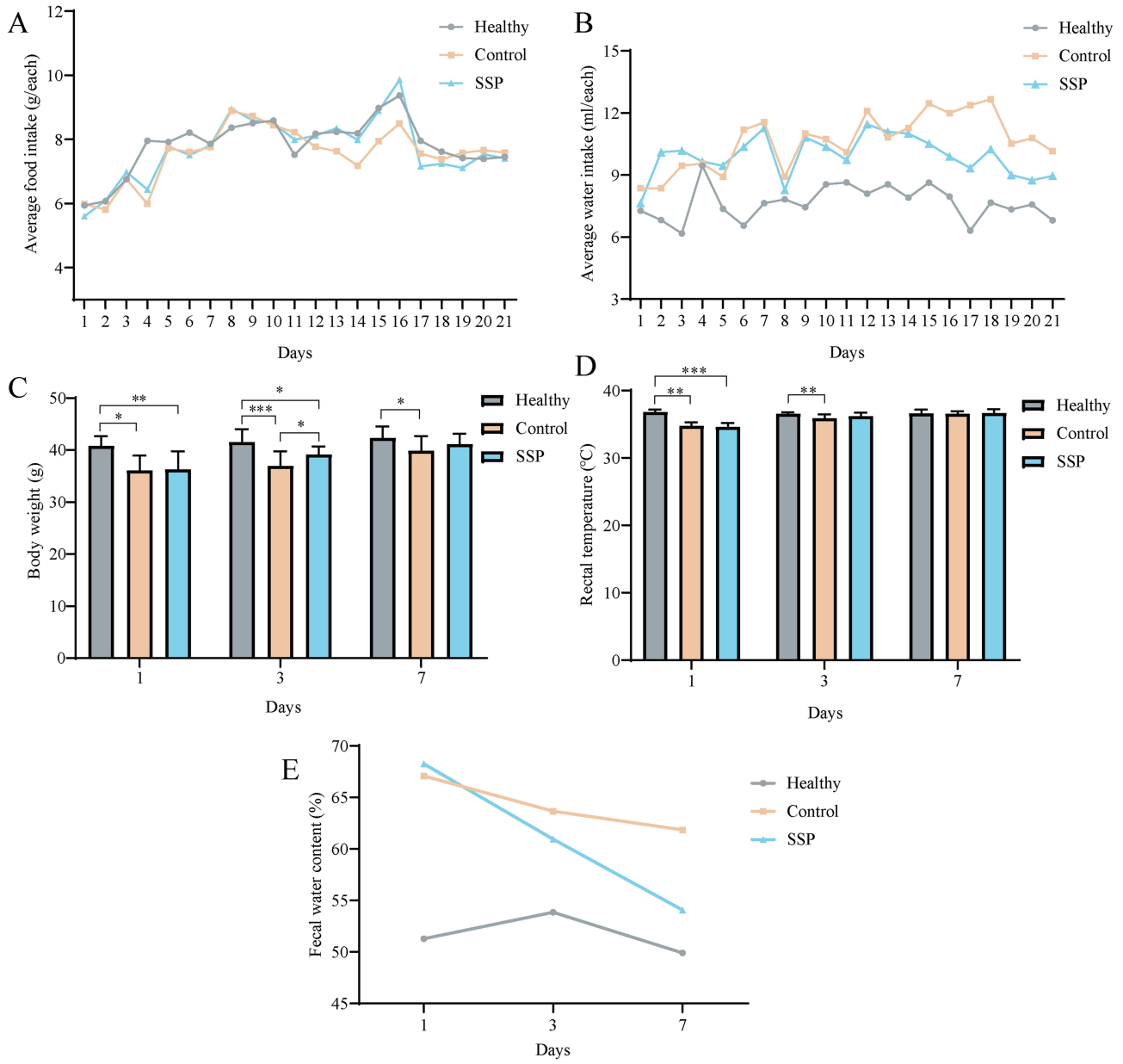

Figure 3 Effects of SSP on General Behavior in Diarrhea with Kidney-Yang Deficiency Syndrome Mice. (**A**) Average food intake. (**B**) Average water intake. (**C**) Body weight. (**D**) Rectal temperature. (**E**) Fecal water content. *p<0.05; **p<0.01; ***p<0.001.

SSP group mice began to decline, falling below the daily average water intake of the Control group. It can be seen that the SSP decoction does not significantly improve the food intake and water consumption of mice with diarrhea with kidney-yang deficiency syndrome.

Comparing the changes in body weight and rectal temperature on days 1, 3, and 7 of SSP treatment. As shown in Figure 3C, on the first day of SSP treatment, compared to the Healthy group, the body weight of mice in the Control group significantly decreased (p<0.05), and the SSP group mice's body weight decreased significantly (p<0.01). On the third day of SSP treatment, compared to the Healthy group, the body weight of mice in the Control group significantly decreased (p<0.001), and the SSP group mice's body weight decreased significantly (p<0.05), but the SSP group mice's body weight was significantly higher than that of the Control group (p<0.05). On the seventh day of treatment, only the body weight of mice in the Control group was significantly lower than that of the Healthy group (p<0.05), while there was no significant difference in body weight between the SSP group and the Healthy group (p>0.05). As shown in

Figure 3D, on the first day of SSP treatment, compared to the Healthy group, the rectal temperature of mice in the Control group significantly decreased ($p<0.01$), and the SSP group mice's rectal temperature also decreased significantly ($p<0.001$). On the third day of SSP treatment, the rectal temperature of mice in the Control group was significantly lower than that of the Healthy group ($p<0.01$), and there was no significant difference in rectal temperature between the SSP group and the Healthy group ($p>0.05$). On the seventh day of SSP treatment, there was no significant difference in rectal temperature among the three groups of mice. This indicates that SSP can promote the recovery of body weight in mice but does not have a significant restorative effect on rectal temperature. It suggests that the SSP decoction can increase the body weight and rectal temperature of mice with diarrhea, gradually restoring them to normal levels.

Compare the changes in fecal water content on days 1, 3, and 7 of SSP treatment. As shown in Figure 3E, on the first day of treatment, the fecal water content of mice in the Control and SSP groups was significantly higher than that in the Healthy group. On the third and seventh days of SSP treatment, there was a sharp decline in fecal water content in the SSP group, while the Healthy group showed a relatively gradual decrease. This suggests that the SSP decoction can, to some extent, reduce the fecal water content in mice with diarrhea.

Effects of SSP on CutC Activity and TMAO Levels in Diarrhea with Kidney-Yang Deficiency Syndrome Mice

As shown in Figure 4A, the serum TMAO level in the Control group was significantly higher than that in the Healthy group ($p<0.01$), while there was no significant difference in TMAO levels between the SSP group and the Healthy group.

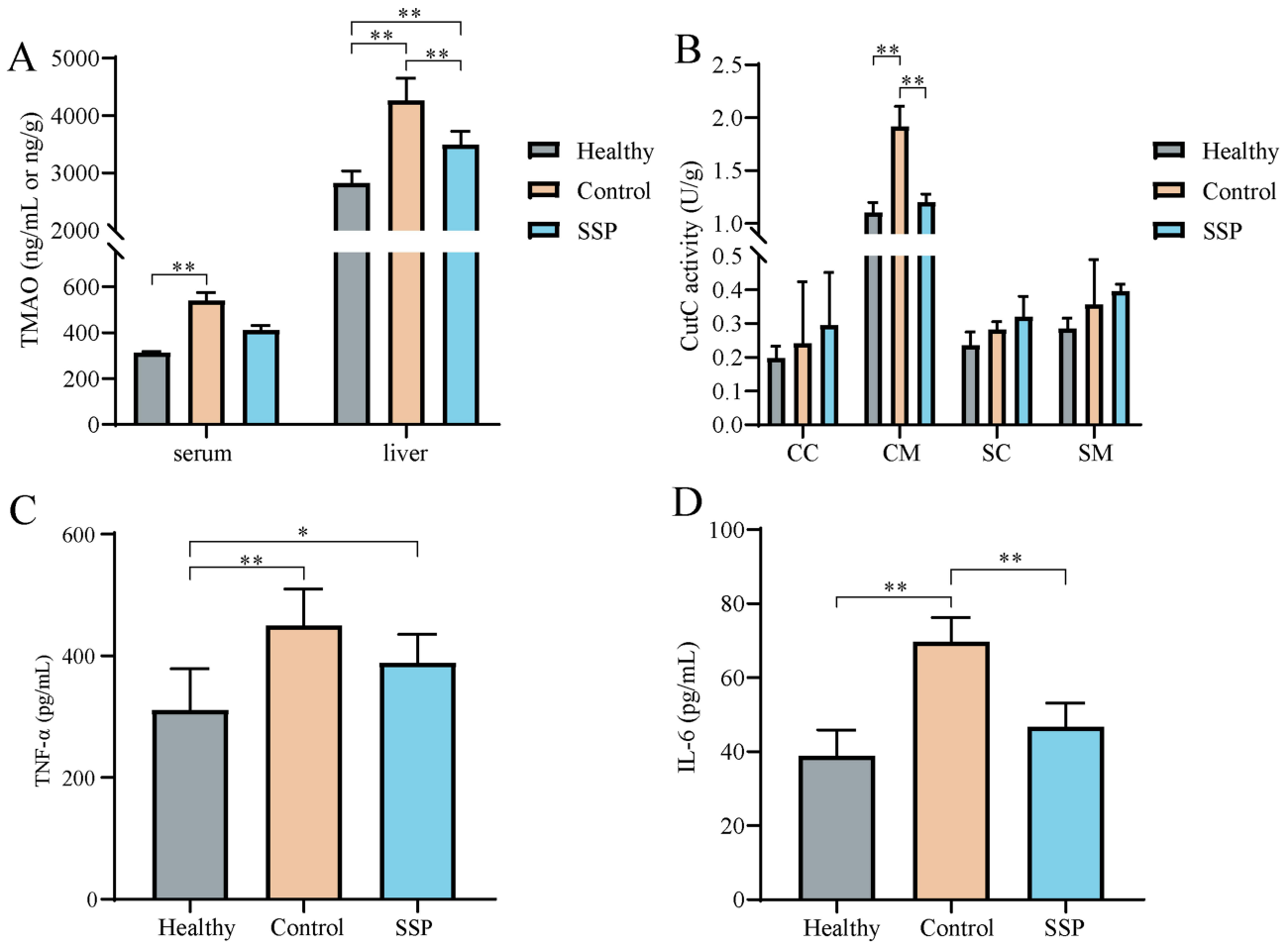

Figure 4 Effects of SSP on CutC Activity, IL-6, TNF-α, and TMAO Levels in Diarrhea with Kidney-Yang Deficiency Syndrome Mice. (**A**) TMAO levels in serum and liver tissue; (**B**) CutC activity in the intestine; (**C**) TNF-α levels in serum; (**D**) IL-6 levels in serum; SC, small intestinal contents; SM, small intestinal mucosa; CC, cecal contents; CM, cecal mucosa. *$p<0.05$, **$p<0.01$.

The TMAO level in the liver tissue of the Control group was significantly higher than that in the Healthy and SSP groups ($p<0.01$), and the TMAO level in the liver tissue of the SSP group was extremely significantly higher than that in the Healthy group ($p<0.01$). This indicates that the SSP decoction has a significant reducing effect on TMAO levels in the serum and liver tissue, but the TMAO level in the liver tissue still does not decrease to normal levels. As shown in Figure 4B, the CutC activity in the cecum mucosa (CM) of the Control group was extremely significantly higher than that in the Healthy and SSP groups ($p<0.01$). However, there was no significant difference in CutC activity in cecal contents (CC), small intestine mucosa (SM), and small intestine contents (SC) among the three groups. This suggests an elevation in CutC activity in the cecum mucosa of mice with diarrhea with kidney-yang deficiency syndrome, and SSP can reduce CutC activity in the cecum mucosa.

Effects of SSP on Serum Levels of IL-6 and TNF-α in Diarrhea with Kidney-Yang Deficiency Syndrome Mice

As shown in Figure 4C, the serum TNF-α level in the Healthy group mice was significantly lower than that in the SSP group ($p<0.05$) and extremely significantly lower than that in the Control group ($p<0.01$). In Figure 4D, the serum IL-6 level in the Control group mice was significantly higher than that in the Healthy and SSP groups ($p<0.01$), while there was no significant difference in serum IL-6 levels between the SSP group and the Healthy group. This suggests that diarrhea with kidney-yang deficiency syndrome can lead to an increase in inflammatory cytokine levels, and SSP has the effect of reducing the levels of inflammatory cytokines.

Effects of SSP on the Richness and Diversity of Cecal Microbiota in Diarrhea with Kidney-Yang Deficiency Syndrome Mice

The dilution curve is mainly used to evaluate whether the sequencing depth is reasonable, indirectly reflecting the richness of species in the sample. With the increase in sample sequencing depth, the dilution curve no longer significantly rises and tends to a plateau, indicating that the sequencing depth of the two groups has covered almost all species in the sample (Figure 5A and B). The species accumulation curve can be used to judge whether the sample size is sufficient. As shown in Figure 5C, with the increase in sample size, the total number of ASVs will no longer significantly increase with the increase in sample size, and the curve tends to flatten, indicating that the sample size in this study is sufficient to reflect the species composition of the community.

The petal chart (Figure 5D) shows that the number of shared ASVs among the Healthy, Control, and SSP groups is 733, while the number of unique ASVs for each group is 2296, 2174, and 1836, respectively.

Alpha diversity reflects the richness and diversity of species in a single sample. Chao1 and Observed_species indices were used to evaluate species richness, and Shannon and Simpson indices were used to evaluate species diversity. As shown in the Figure 5E and F, there were no significant changes in the Chao1 index ($p=0.78$) and Observed species ($p=0.83$) among the three groups. Compared to the Healthy group, the Shannon index ($p=0.34$) (Figure 5G) and Simpson index ($p=0.23$) (Figure 5H) in the Control group increased, while the Shannon and Simpson indices in the SSP group showed a decreasing trend compared to the Healthy group, but the differences were not statistically significant. This suggests that the alpha diversity of the internal microbiota changed during the modeling process, manifested by a decreasing trend in both richness and diversity of the cecal microbiota in mice. Beta diversity focuses on differences between samples. PCoA unfolds the sample distance matrix in a low-dimensional space, preserving the original distance relationships of the samples to the maximum extent, in line with the characteristics of ecological data. In Figure 5I, the contribution rates of PCo1 and PCo2 are 11.4% and 10.1% on the x-axis and y-axis, respectively. There is no intersection between the Healthy and Control groups, and they show a grouping clustering phenomenon, indicating that diarrhea with kidney-yang deficiency syndrome changes the microbial community structure of cecal contents. The SSP group intersects with the Healthy group, suggesting that SSP favors the recovery of microbial community structure towards the Healthy group.

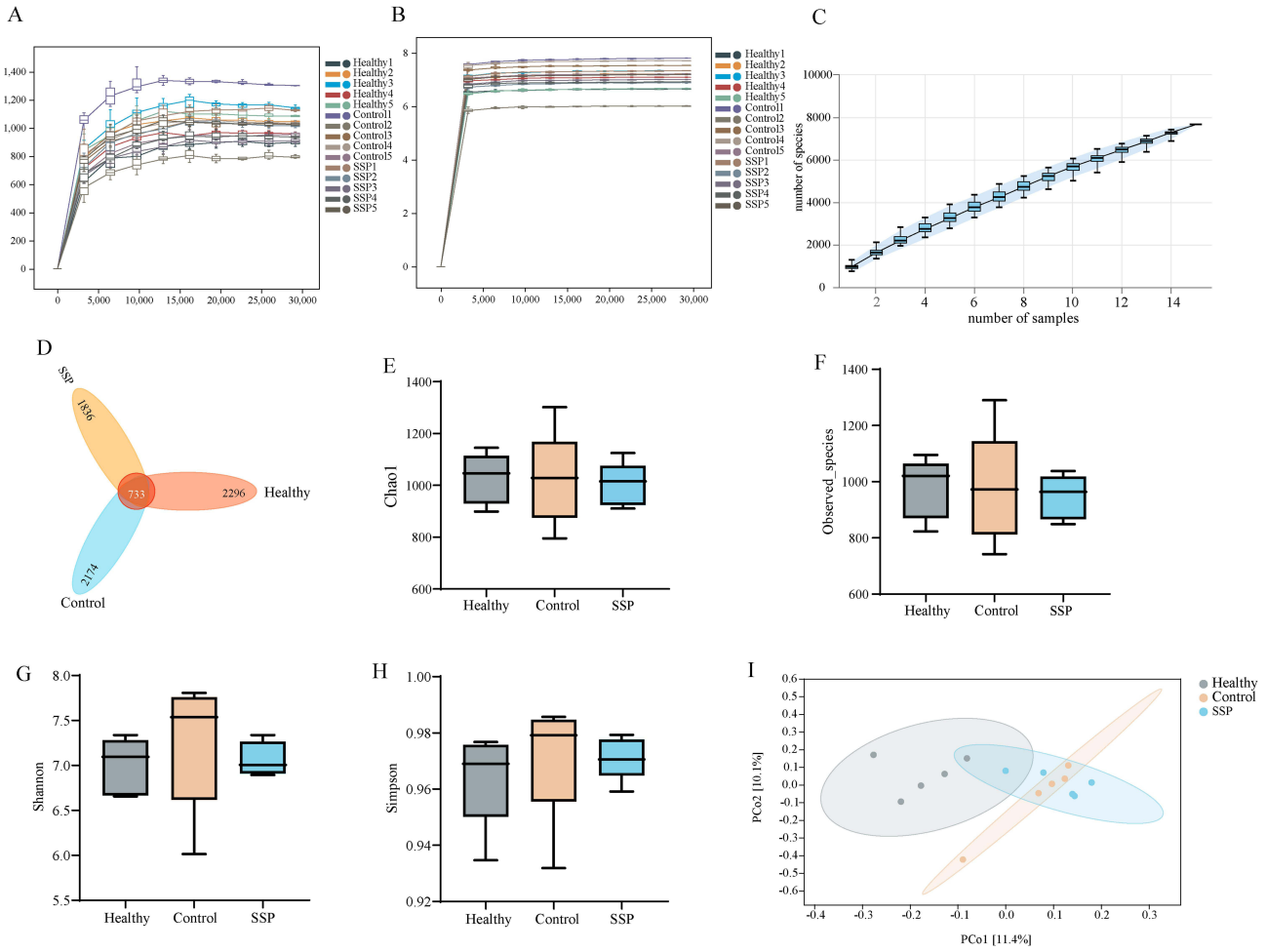

Figure 5 Effects of SSP on the Abundance and Diversity of ASVs in the Cecal Microbiota of Diarrhea with Kidney-Yang Deficiency Syndrome Mice. (**A**) Chao1 rarefaction curve; (**B**) Shannon rarefaction curve; (**C**) Species accumulation curve; (**D**) Number of ASVs; (**E**) Chao1 index; (**F**) Observed_species index; (**G**) Shannon index; (**H**) Simpson index; (**I**) Principal Coordinates Analysis.

Effects of SSP on the Dominant Microbial Community in the Cecal Contents of Diarrhea with Kidney-Yang Deficiency Syndrome Mice

Figure 6A displays the relative abundance of the top 10 phyla in the cecal microbiota. Firmicutes is the major dominant phylum in all groups, accounting for 48.82%, 38.06%, and 55.23% in the Healthy, Control, and SSP groups, respectively. Bacteroidetes is the second major phylum, with proportions of 44.13%, 53.20%, and 37.78%, respectively. Desulfobacterota is the third major phylum, with proportions of 2.42%, 3.16%, and 1.61%, respectively. At the genus level (Figure 6B), the dominant genera in each group are *Muribaculaceae*, accounting for 26.64%, 19.85%, and 26.24% in the Healthy, Control, and SSP groups, respectively. The second major genus is *Lachnospiraceae_NK4A136_group*, with proportions of 8.43%, 11.77%, and 6.85%, respectively. Additionally, *Alistipes* has a higher abundance in the Healthy group, accounting for 11.90%, while *Odoribacter* has a higher abundance in the SSP group, accounting for 10.07%. Subsequently, statistical analysis of the above species (Figure 6C–F) revealed that the relative abundance of the phylum Bacteroidetes in the cecal contents of mice in the SSP group was significantly higher than that in the Control group ($p<0.05$), and the relative abundance of the phylum Firmicutes was significantly lower than that in the Control group ($p<0.05$). However, there was no significant difference in the ratio of Firmicutes to Bacteroidetes (F/B ratio) among the three groups ($p>0.05$). Compared to the Healthy group, the abundance of the genus *Odoribacter* in the cecal contents of mice in the Control and SSP groups increased significantly ($p<0.05$).

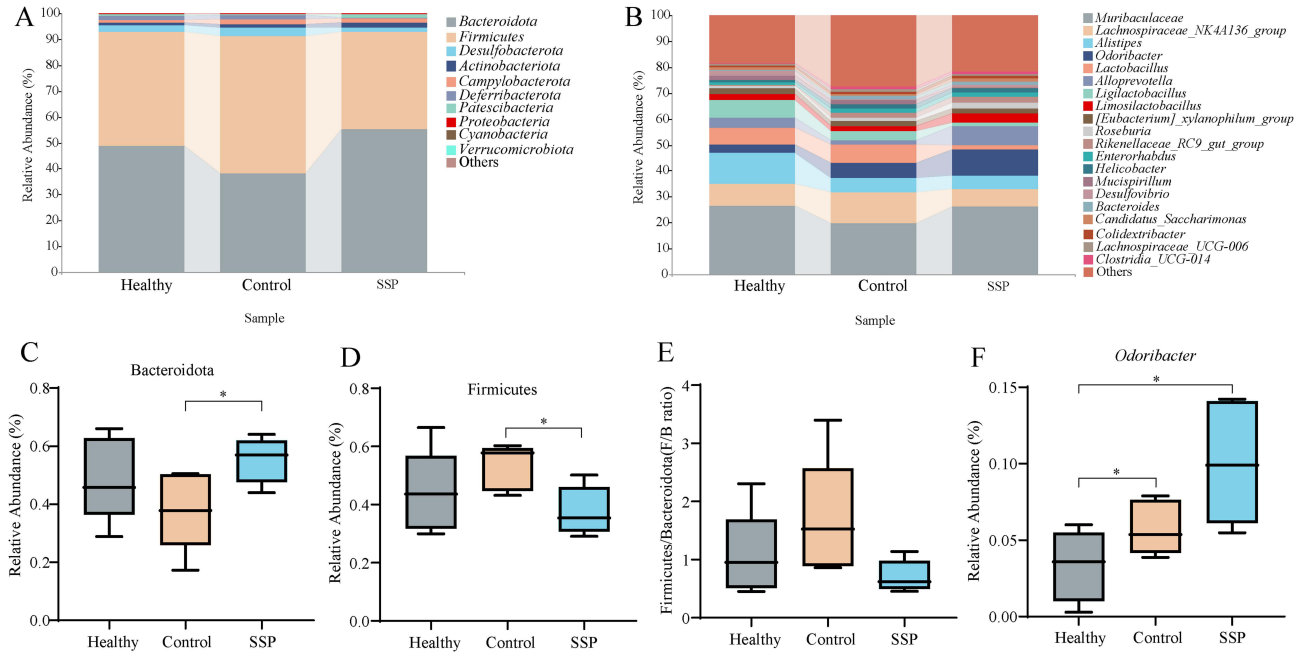

Figure 6 Effects of SSP on the Dominant Microbial Community in the Cecal Contents of Diarrhea with Kidney-Yang Deficiency Syndrome Mice. (**A**) Relative abundance plot at the phylum level; (**B**) Relative abundance plot at the genus level; (**C** and **D**) Dominant phyla; (**E**) F/B ratio; (**F**) Dominant genera. *p<0.05.

Effects of SSP on the Characteristic Microbiota in the Cecal Contents of Diarrhea with Kidney-Yang Deficiency Syndrome Mice

LEfSe analysis was conducted with a threshold set at >3.0 to identify taxa with significant differences in sample division between groups, focusing on the characteristic taxa between Healthy and Control groups, as well as Control and SSP groups. The LEfSe analysis between Healthy and Control groups (Figure 7A) revealed significant enrichment of *Prevotellaceae_UCG_001* (LDA=3.71; *p*=0.016), *Ruminococcaceae* (LDA=3.45; *p*=0.026), *Eubacterium_siraeum_group* (LDA=3.35; *p*=0.018) and *Acinetobacter* (LDA=3.31; *p*=0.034) in the Healthy group, while *Rikenellaceae_RC9_gut_group* (LDA=3.90; *p*=0.028), *A2* (LDA=3.62; *p*=0.047), *Chryseobacterium* (LDA=3.36; *p*=0.005), *Candidatus_Arthromitus* (LDA=3.28; *p*=0.018), and *Faecalibaculum* (LDA=3.27; *p*=0.023) were significantly enriched in the Control group. In the LEfSe analysis between Control and SSP groups (Figure 7B), *Chryseobacterium* (LDA=3.95; *p*=0.005) and *A2* (LDA=3.71; *p*=0.047) were significantly enriched in the Control group, whereas *Alloprevotella* (LDA=4.47; *p*=0.016), *Desulfovibrio* (LDA=3.29; *p*=0.047), *Ruminococcus* (LDA=3.21; *p*=0.047), *Prevotellaceae_UCG_001* (LDA=3.17; *p*=0.047), and *Parasutterella* (LDA=3.15; *p*=0.044) were significantly enriched in the SSP group.

To further analyze the impact of SSP on the cecal contents of mice with diarrhea with kidney-yang deficiency syndrome, a random forest model (Figure 7C and D) was established to screen the top 10 important bacteria in Healthy, Control, and SSP groups. ROC analysis was then conducted, with an AUC>0.8 as the standard, to validate the accuracy of the combined evaluation of diagnostic and characteristic bacteria between different groups and determine their diagnostic and therapeutic efficacy. The bacteria with AUC>0.8 were defined as important bacteria describing different features between the two groups. In the ROC analysis between Healthy and Control groups (Figure 7E), the bacteria with AUC>0.8 were *Faecalibaculum* (AUC=0.920), *Family_XIII_UCG−001* (AUC=0.880), *Lacticaseibacillus* (AUC=0.900), *Prevotellaceae_UCG−001* (AUC=0.960), *Acinetobacter* (AUC=0.880), *Rikenella* (AUC=0.960), and *[Eubacterium]_siraeum_group* (AUC=0.900). Similarly, in the ROC analysis between Control and SSP groups (Figure 7F), specific bacterial taxa exhibited prominent AUC values: *Chryseobacterium* (AUC=1.000), *Parasutterella* (AUC=0.880), *A2* (AUC=0.880), *Prevotellaceae_UCG−001* (AUC=0.880), and *Odoribacter* (AUC=0.840). Among them, *Faecalibaculum, Family_XIII_UCG−001, Lacticaseibacillus, Prevotellaceae_UCG−001, Acinetobacter, Rikenella, [Eubacterium]_siraeum_group, Chryseobacterium, Parasutterella, A2*, and *Odoribacter* all had AUC values >0.8, suggesting that they are bacteria with diagnostic efficacy.

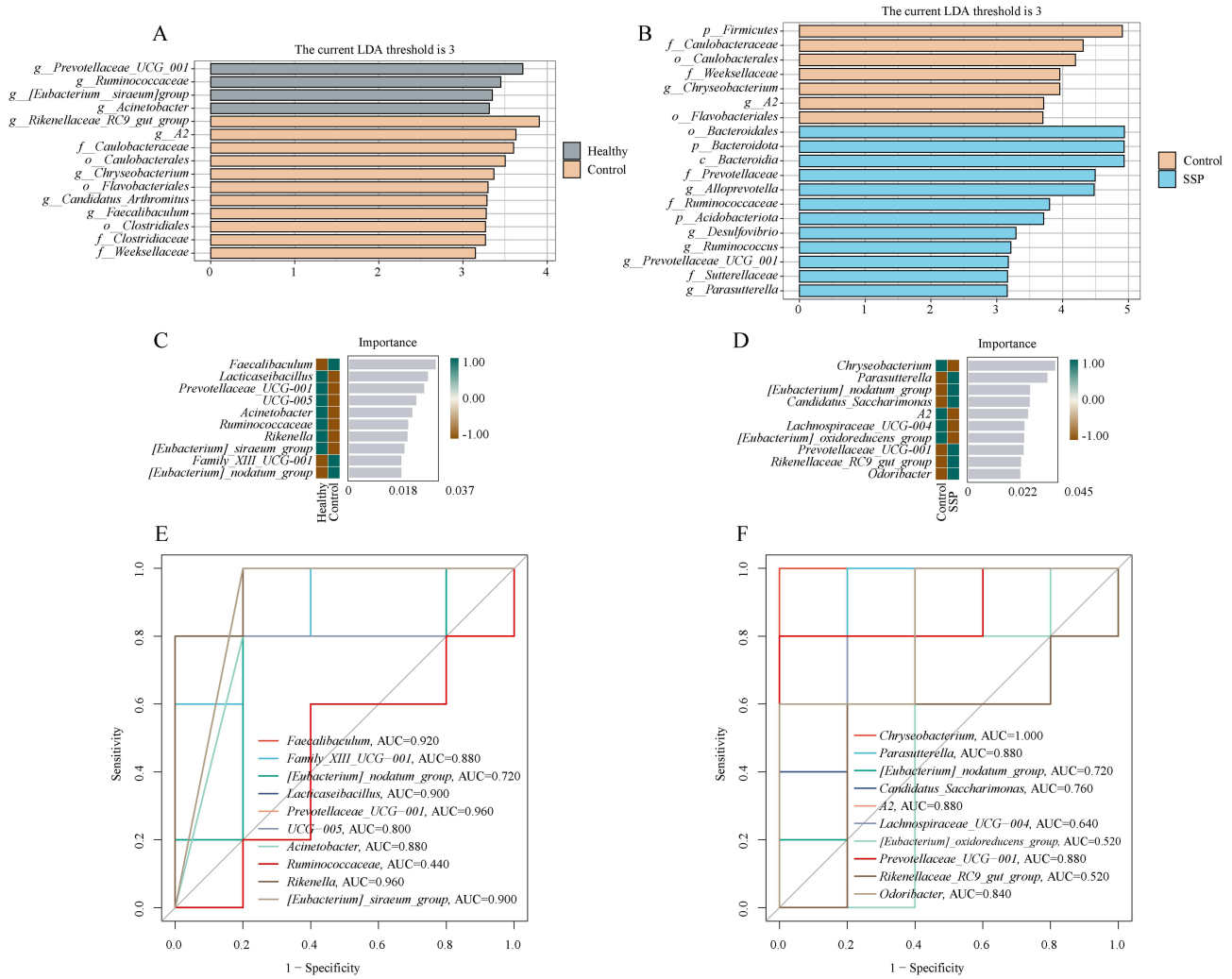

Figure 7 Effects of SSP on the Characteristic Microbiota in the Cecal Contents of Diarrhea with Kidney-Yang Deficiency Syndrome Mice. (**A**) Distribution of LDA scores (Healthy vs Control); (**B**) Distribution of LDA scores (Control vs SSP); (**C**) Genus-level random forest plot (Healthy vs Control); (**D**) Genus-level random forest plot (Control vs SSP); (**E**) Genus-level ROC curve (Healthy vs Control); (**F**) Genus-level ROC curve (Control vs SSP).

Correlation Analysis of SSP in the Treatment of Diarrhea with Kidney-Yang Deficiency Syndrome

To explore the relationship between SSP treatment for diarrhea with kidney-yang deficiency syndrome, CutC activity, cecal microbial community, TMAO, and inflammatory factors, random forest analysis was conducted. The top 10 feature genera were selected for Healthy vs Control groups and Control vs SSP groups. Spearman correlation analysis was performed directly between these genera and CutC activity. In the analysis of the top 10 feature genera in Healthy and Control groups (Figure 8A), CutC activity in cecal mucosa (CM) was significantly negatively correlated with *Prevotellaceae_UCG−001* ($p<0.05$), *Rikenella* ($p<0.05$), *Acinetobacter* ($p<0.05$), and *Lacticaseibacillus* ($p<0.01$). In the analysis of the top 10 feature genera in Control and SSP groups (Figure 8B), CutC activity in cecal mucosa was significantly negatively correlated with *Parasutterella* ($p<0.05$) and significantly positively correlated with *Chryseobacterium* ($p<0.05$). Subsequently, Spearman correlation analysis was conducted between the top 10 feature genera and the levels of TNF-α, IL-6, and TMAO. In the analysis between Healthy and Control groups (Figure 8C), serum TNF-α level was significantly negatively correlated with *Lacticaseibacillus* ($p<0.05$) and *Prevotellaceae_UCG−001* ($p<0.01$). Serum IL-6 level was significantly negatively correlated with *Rikenella* ($p<0.05$), *Acinetobacter* ($p<0.05$), *Prevotellaceae_UCG−001* ($p<0.05$), and *Lacticaseibacillus* ($p<0.01$), and significantly positively correlated with *Faecalibaculum* ($p<0.05$). Liver TMAO level was significantly negatively correlated with *Rikenella* ($p<0.05$), *Prevotellaceae_UCG−001* ($p<0.05$), and *[Eubacterium]_siraeum_group*

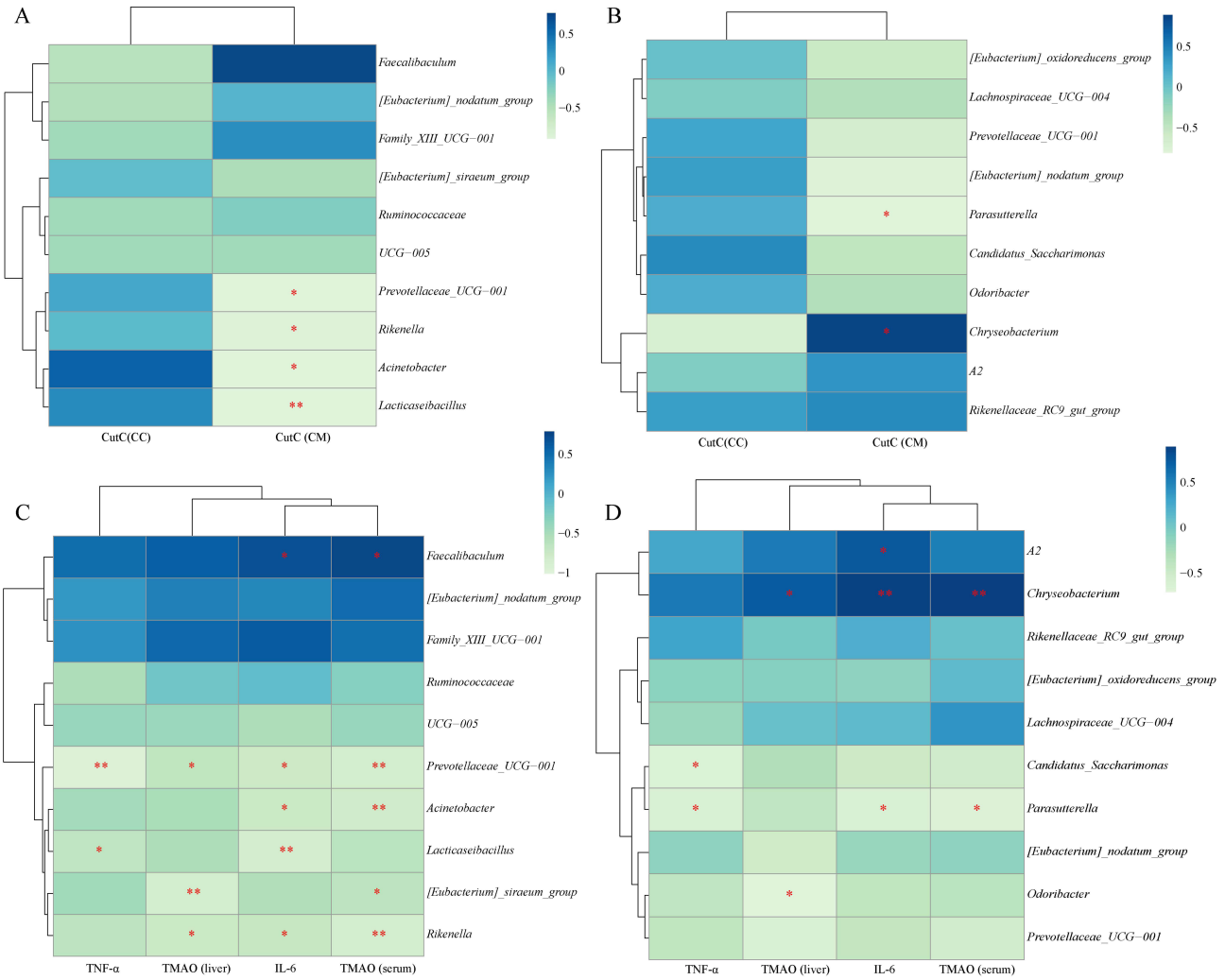

Figure 8 Correlation heatmaps between characteristic bacteria and CutC activity: (**A**) Healthy and Control; (**B**) Control and SSP. Correlation heatmaps between characteristic bacteria, TMAO, and inflammatory factors: (**C**) Healthy and Control; (**D**) Control and SSP. CC: Cecal contents. CM: Cecal mucosa. *$p<0.05$, **$p<0.01$.

($p<0.01$). Serum TMAO level was significantly negatively correlated with *[Eubacterium]_siraeum_group* ($p<0.05$), *Rikenella* ($p<0.01$), *Acinetobacter* ($p<0.01$), and *Prevotellaceae_UCG−001* ($p<0.01$), and significantly positively correlated with *Faecalibaculum* ($p<0.05$). In the analysis between Control and SSP groups (Figure 8D), serum TNF-α level was significantly negatively correlated with *Parasutterella* ($p<0.05$) and *Candidatus_Saccharimonas* ($p<0.05$). Serum IL-6 level was significantly negatively correlated with *Parasutterella* ($p<0.05$) and significantly positively correlated with *Chryseobacterium* ($p<0.01$) and *A2* ($p<0.05$). Liver TMAO level was significantly negatively correlated with *Odoribacter* ($p<0.05$) and significantly positively correlated with *Chryseobacterium* ($p<0.05$). Serum TMAO level was significantly negatively correlated with *Parasutterella* ($p<0.05$) and significantly positively correlated with *Chryseobacterium* ($p<0.01$).

Effects of SSP on the Functional Profile of Cecal Microbial Community in Diarrhea with Kidney-Yang Deficiency Syndrome Mice

Based on the PICRUSt2 analysis using the KEGG database, the functional categories of the cecal microbial community are generally divided into six classes (Figure 9A), mainly including Organismal Systems, Metabolism, Human Diseases, Genetic Information Processing, Environmental Information Processing, and Cellular Processes. Among them, the metabolic pathways of Metabolism, Genetic Information Processing, Environmental Information Processing, and Cellular Processes have a higher abundance. The second level includes 35 sub-functional categories. In the Cellular

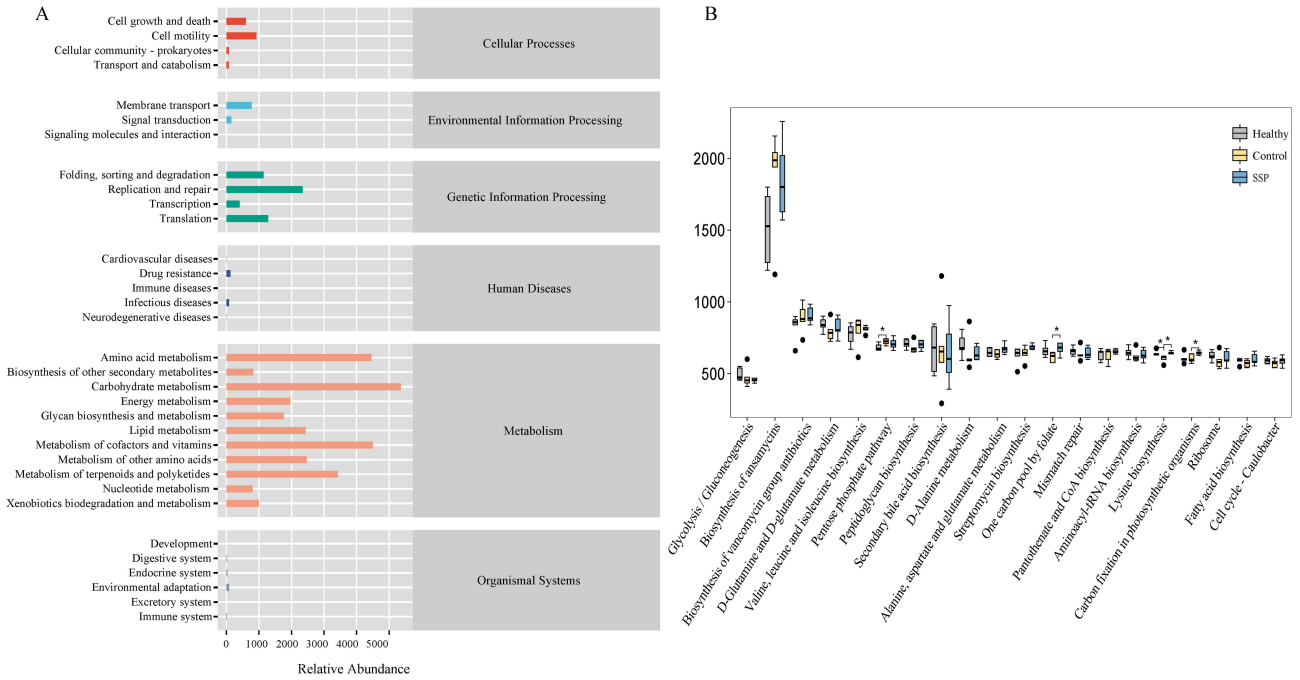

Figure 9 Effects of SSP on the Functional Profile of Cecal Microbial Community in Diar-rhea with Kidney-Yang Deficiency Syndrome Mice. (**A**) Predicted KEGG functional pathways; (**B**) Inter-group comparison of metabolic functions. *p<0.05.

Processes metabolic pathways, the abundance of Cell motility and Cell growth and death is higher. In Environmental Information Processing, the abundance of Membrane transport is higher. In Genetic Information Processing, the metabolic abundance of Translation, Replication and repair, and Folding, sorting, and degradation are higher. In Metabolism, the metabolic pathways of Metabolism of terpenoids and polyketides, Metabolism of other amino acids, Metabolism of cofactors and vitamins, Lipid metabolism, Carbohydrate metabolism, and Amino acid metabolism have higher abundance. Further analysis (Figure 9B) revealed that in the Pentose phosphate pathway, the abundance was significantly upregulated in the Control group compared to the Healthy group (p<0.05). In the One-carbon pool by folate pathway, the abundance was significantly upregulated in the SSP group compared to the Control group (p<0.05). In the Lysine biosynthesis pathway, the abundance was significantly upregulated in both the Healthy and SSP groups compared to the Control group (p<0.05). In the Carbon fixation in photosynthetic organisms pathway, the abundance was significantly upregulated in the SSP group compared to the Control group (p<0.05).

Discussion

SSP Regulate the Cecal Microbiota, a Crucial Factor in Its Therapeutic Effect on Diarrhea with Kidney-Yang Deficiency Syndrome Mice

Our study found that the structure of the cecal microbiota altered in both the Control group and the SSP group. ASV analysis revealed that the model of diarrhea with kidney-yang deficiency syndrome and and SSP intervention led to changes in the cecal microbiota. PCoA demonstrated that both the diarrhea model and SSP intervention affected the cecal microbiota structure. Notably, the cecal microbiota profiles of the SSP and Healthy groups were closely aligned and overlapped, suggesting that SSP could restore the cecal microbiota structure.

SSP altered the relative abundance of major bacterial phyla and genera in the cecum of model mice. Specifically, the relative abundance of Bacteroidota was higher in the SSP group compared to the Control group, while the relative abundance of Firmicutes was lower in the SSP group. The F/B ratio slightly increased in the Control group relative to the Healthy group, but the F/B ratio in the SSP group tended to return towards levels observed in the Healthy group. Firmicutes is the predominant phylum in the cecal microbiota, followed by Bacteroidota.[31] The F/B ratio is crucial for

maintaining intestinal balance; an increased F/B ratio is indicative of ecological imbalance and is often associated with the development of diseases such as cardiovascular disease, obesity, and diabetes.[32,33]

Further LEfSe analysis and ROC analysis of Healthy vs Control groups and Control vs SSP groups revealed meaningful differential species, including *A2, Chryseobacterium*, and *Faecalibaculum* in the Control group. *A2* is an unnamed genus in the Lachnospiraceae family. Studies have reported that *Chryseobacterium* belongs to the Bacteroidetes phylum, and its frequent distribution in patients with coronary artery disease, especially in those with weakened immunity and irrational use of antibiotics, can cause endogenous infections and dominate the intestinal microbiota.[34,35] *Faecalibaculum* has been found to increase in experimental obesity and is positively correlated with serum lipid level.[36] *Alloprevotella, Ruminococcus, Prevotellaceae_UCG_001, Parasutterella*, and *Odoribacter* are meaningful differential bacteria in the SSP group. *Alloprevotella* is usually considered a bacterium related to a healthy plant-based diet and acts as a "probiotic" in the human intestinal tract. *Alloprevotella* is also considered a producer of short-chain fatty acids.[37] Seventy percent of the energy of intestinal epithelial cells comes from butyric acid produced by bacteria in the *Ruminococcus* and *Faecalibacterium* genera.[38] *Prevotellaceae_UCG_001* belongs to the Prevotellaceae family and can produce short-chain fatty acids.[39] *Odoribacter* is considered a beneficial bacterium because it is negatively correlated with the severity of non-alcoholic fatty liver and inflammatory bowel disease. The species Odoribacter splanchnicus can produce SCFAs and has anti-inflammatory activity.[40] *Parasutterella* has been defined as a core component of the intestinal microbiota in humans and mice, promoting host health in the gastrointestinal tract.[41]

In summary, SSP treatment shifts the cecal microbiota composition from a predominance of harmful bacteria, characteristic of the diarrhea model, to a predominance of beneficial bacteria. This shift restores intestinal balance and contributes to the therapeutic efficacy of SSP in treating diarrhea. In addition, further experiments involving fecal microbiota transplantation (FMT) would be significant. Transplanting the fecal microbiota from SSP-treated diarrhea with kidney-yang deficiency syndrome mice into untreated diarrhea with kidney-yang deficiency syndrome mice could further validate the critical role of gut microbiota in SSP treatment. The absence of such FMT experiments is a limitation of this study.

The SSP Can Downregulate CutC Activity in Cecal Mucosa, Decrease the Expression of TMAO and Inflammatory Factor

Our study demonstrated that neither diarrhea nor SSP intervention significantly altered CutC activity in the cecal contents or small intestine mucosa. However, in the cecal mucosa, CutC activity was elevated in the Control group, indicating dysregulated TMA metabolism associated with diarrhea. Notably, SSP treatment effectively normalized CutC activity to levels comparable to the Healthy group, indicating its potential in restoring microbial homeostasis. CutC, produced by the intestinal microbiota, is pivotal in TMA production from choline and plays a crucial role in conditions associated with dysbiosis.[13,42,43] Through anaerobic degradation of choline, CutC initiates the conversion of choline to TMA via a glycine radical-mediated mechanism, ultimately leading to TMAO formation in the liver.[44,45] TMAO, implicated in diseases such as atherosclerosis and chronic kidney disease, exerts pathogenic effects by inducing the expression of inflammatory factors, including IL-1β, IL-6, and TNF-α.[46,47]

Consistent with the modulation of CutC activity, TMAO levels in serum and liver were elevated in the Control group compared to the Healthy group, reflecting dysbiosis-induced metabolic disturbances. Remarkably, SSP intervention attenuated TMAO accumulation in serum, suggesting a regulatory effect on TMA metabolism. These findings underscore the therapeutic potential of SSP decoction in mitigating TMAO-related health risks. Furthermore, our study assessed the impact of SSP intervention on inflammatory cytokines TNF-α and IL-6, which are implicated in chronic low-grade inflammatory diseases. Elevated levels of TNF-α and IL-6 in the Control group suggested an inflammatory response associated with dysbiosis-induced TMAO accumulation. Importantly, SSP treatment mitigated TNF-α elevation and restored IL-6 levels to baseline, highlighting its anti-inflammatory potential.

In conclusion, our findings demonstrate that SSP treatment effectively modulates CutC activity, reduces TMAO levels, and attenuates inflammatory cytokine expression, thereby ameliorating diarrhea-associated dysbiosis and its systemic complications. Although this study highlights the regulatory effects of SSP, it lacks an in-depth exploration of the specific molecular mechanisms involved. Further investigation into the molecular mechanisms underlying SSP's effects on the cecal microbiota and host metabolism is necessary to optimize its therapeutic application.

Distinct Cecal Microbiota Correlate with CutC Activity, TMAO Levels, and Inflammatory Factors, Highlighting Their Role in SSP-Mediated Therapeutic Effects

In our study, significant correlations emerged between CutC activity and cecal microbiota. *Faecalibaculum* and *Chryseobacterium* correlated positively with CutC activity, while *Prevotellaceae UCG−001, Rikenella, Acinetobacter, Parasutterella*, and *Lacticaseibacillus* showed negative correlations, indicating microbiota influence on CutC activity. Moreover, changes in CutC activity aligned with TMAO level trends. *Faecalibaculum* and *Chryseobacterium* not only correlated positively with CutC activity but also with TNF-α, IL-6, and TMAO levels, suggesting a link between CutC activity and TMAO production. Additionally, TMAO levels correlated with inflammatory factors. *Prevotellaceae UCG−001, Rikenella, Acinetobacter, Parasutterella*, and *Lacticaseibacillus* displayed negative correlations with both CutC activity and TNF-α, IL-6, and TMAO levels, indicating a potential association between TMAO levels and inflammation.

Faecalibaculum is positively correlated with TMAO, and studies have shown that chlorogenic acid (CGA) reduces TMAO production by regulating intestinal microbiota involved in TMAO synthesis, such as *Blautia, Enterococcus*, and *Faecalibaculum*. This regulation lowers the risk of renal fibrosis and demonstrates potential in preventing hyperuricemic nephropathy.[48] Our results confirmed that *Faecalibaculum* promotes TMAO production, which is associated with enhanced CutC enzyme activity. *Chryseobacterium*, an opportunistic pathogen, produces unique sphingolipids called sulfolipids (SoL) that promote inflammation.[49] However, its relationship with CutC enzymatic activity remains unclear.

Studies have found that homologs of the CutC gene are present in the genomes of 89 bacterial species. These homologs are unevenly distributed among the major bacterial phyla in the gut, primarily found in Firmicutes, Actinobacteria, and Proteobacteria.[50] Additionally, Desulfovibrio is one of the top five genera in humans carrying CutC.[43] Knocking out the CutC gene in Desulfovibrio desulfuricans results in the loss of its ability to convert choline to TMA (which is further converted to TMAO).[50] This indicates that changes in CutC are indeed caused by the intestinal microbiota. The presence of the CutC gene directly affects TMA production, which can be converted to TMAO in the liver. Researchers inoculated germ-free mice with either wild-type MS 200–1 strains or CutC gene mutant MS 200–1 strains. After induction with a high-fat diet, mice inoculated with the wild-type strain showed significantly elevated TMAO levels in their blood compared to those inoculated with the mutant strain.[51] This demonstrates a close correlation between CutC activity and TMAO levels. TMAO can upregulate the expression of inflammatory factors such as TNF-α and IL-6 by activating p38 phosphorylation and upregulating human antigen R, thereby contributing to the development of cardiovascular diseases and chronic kidney disease. Injecting TMAO into female LDL C57BL/6J mice and treating cultured HAECs and VSMCs with this molecule resulted in higher IL-6 mRNA expression levels in the aorta and cells, respectively.[52] It can be concluded that the cecal microbiota-CutC-TMAO-inflammatory factor axis may be a potential mechanism for the occurrence of diarrhea.

Conclusion

In conclusion, our study indicates that SSP significantly alleviates symptoms of diarrhea with kidney-yang deficiency syndrome. SSP achieves this by downregulating CutC activity, reducing TMAO levels, and decreasing inflammatory cytokines such as TNF-α and IL-6. These effects are mediated through modulation of the cecal microbiota, specifically by reducing harmful bacteria (*Faecalibaculum* and *Chryseobacterium*) and increasing beneficial bacteria (*Prevotellaceae* UCG −001, *Rikenella*, etc). The cecal microbiota-CutC-TMAO-inflammatory cytokine axis may be a key mechanism underlying SSP's therapeutic effects on diarrhea with kidney-yang deficiency syndrome. These findings enhance our understanding of the mechanisms by which SSP exerts its therapeutic effects.

Abbreviations

SSP, Sishen Pill; TCM, traditional Chinese medicine; TMAO, trimethylamine N-oxide; CutC, choline-trimethylamine lyase; TMA, trimethylamine; FMOs, flavin-containing monooxygenases; ELISA, enzyme-linked immunosorbent assay; ASVs, amplicon sequence variants; PCoA, principal coordinate analysis; LEfSe, linear discriminant analysis effect size; Healthy, the normal control group; Control, the model control group; FMT, fecal microbiota transplantation.

Data Sharing Statement

The datasets presented in this study can be found in online repositories. The names of the repository/repositories and accession number(s) can be found at: https://www.ncbi.nlm.nih.gov/, PRJNA1073021.

Ethics Approval and Informed Consent

The experiment was approved by the Animal Ethics and Welfare Committee of Hunan University of Chinese Medicine and was conducted in accordance with the Guidelines for Humane Endpoint Review of Animal Experiments. (Ethics Number: LL2023081010).

Acknowledgments

This research received no specific grant from any funding agency in the public, commercial, or not-for-profit sectors.

Disclosure

The authors report no conflicts of interest in this work.

References

1. Schiller LR, Pardi DS, Sellin JH. Chronic diarrhea: diagnosis and management. *Clin Gastroenterol Hepatol*. 2017;15(2):182–193.e3. doi:10.1016/j.cgh.2016.07.028
2. Zhu J, Li X, Deng N, Peng X, Tan Z. Diarrhea with deficiency kidney-yang syndrome caused by adenine combined with Folium senna was associated with gut mucosal microbiota. *Front Microbiol*. 2022;13:1007609. doi:10.3389/fmicb.2022.1007609
3. Zhu J, Li X, Deng N, et al. Intestinal mucosal flora of the intestine-kidney remediation process of diarrhea with deficiency kidney-yang syndrome in Sishen pill treatment: association with interactions between Lactobacillus johnsonii, Ca^{2+}-Mg^{2+}-ATP-ase, and Na^{+}-K^{+}-ATP-ase. *Heliyon*. 2023;9(5):e16166. doi:10.1016/j.heliyon.2023.e16166
4. Li X, Peng X, Qiao B, et al. Gut-kidney impairment process of adenine combined with Folium sennae-induced diarrhea: association with interactions between Lactobacillus intestinalis, bacteroides acidifaciens and acetic acid, inflammation, and kidney function. *Cells*. 2022;11(20):3261. doi:10.3390/cells11203261
5. Xu J, Liu C, Shi K, et al. Atractyloside-A ameliorates spleen deficiency diarrhea by interfering with TLR4/MyD88/NF-κB signaling activation and regulating intestinal flora homeostasis. *Int Immunopharmacol*. 2022;107:108679. doi:10.1016/j.intimp.2022.108679
6. Sun T, Liu X, Su Y, et al. The efficacy of anti-proteolytic peptide R7I in intestinal inflammation, function, microbiota, and metabolites by multi-omics analysis in murine bacterial enteritis. *Bioeng Transl Med*. 2023;8(2):e10446. doi:10.1002/btm2.10446
7. Wang H, Yao J, Chen Y, et al. Gut dysbacteriosis attenuates resistance to Mycobacterium bovis infection by decreasing cyclooxygenase 2 to inhibit endoplasmic reticulum stress. *Emerg Microbes Infect*. 2022;11(1):1806–1818. doi:10.1080/22221751.2022.2096486
8. Sakai K, Sakurai T, De Velasco MA, et al. Intestinal microbiota and gene expression reveal similarity and dissimilarity between immune-mediated colitis and ulcerative colitis. *Front Oncol*. 2021;11:763468. doi:10.3389/fonc.2021.763468
9. Shao H, Zhang C, Xiao N, Tan Z. Gut microbiota characteristics in mice with antibiotic-associated diarrhea. *BMC Microbiol*. 2020;20(1):313. doi:10.1186/s12866-020-01999-x
10. Guo M, Fang L, Chen M, Shen J, Tan Z, He W. Dysfunction of cecal microbiota and CutC activity in mice mediating diarrhea with kidney-yang deficiency syndrome. *Front Microbiol*. 2024;15:1354823. doi:10.3389/fmicb.2024.1354823
11. Beker BM, Colombo I, Gonzalez-Torres H, Musso CG. Decreasing microbiota-derived uremic toxins to improve CKD outcomes. *Clin Kidney J*. 2022;15(12):2214–2219. doi:10.1093/ckj/sfac154
12. Wang Z, Klipfell E, Bennett BJ, et al. Gut flora metabolism of phosphatidylcholine promotes cardiovascular disease. *Nature*. 2011;472(7341):57–63. doi:10.1038/nature09922
13. Wang Z, Roberts AB, Buffa JA, et al. Non-lethal inhibition of gut microbial trimethylamine production for the treatment of atherosclerosis. *Cell*. 2015;163(7):1585–1595. doi:10.1016/j.cell.2015.11.055
14. Messenger J, Clark S, Massick S, Bechtel M. A review of trimethylaminuria: (fish odor syndrome). *J Clin Aesthet Dermatol*. 2013;6(11):45–48.
15. Chen S, Hao M, Zhang L. Antidiarrheal effect of fermented Millet Bran on diarrhea induced by Senna leaf in mice. *Foods*. 2022;11(14):2082. doi:10.3390/foods11142082
16. Liu L, Wang S, Xu QX, Xu W, Zhang YB, Yang XW. Poly-pharmacokinetic strategy represented the synergy effects of bioactive compounds in a traditional Chinese medicine formula, Si Shen Wan and its separated recipes to normal and colitis rats. *J Sep Sci*. 2021;44(10):2065–2077. doi:10.1002/jssc.202001258
17. Ge W, Zhou BG, Zhong YB, et al. Sishen Pill ameliorates dextran sulfate sodium (DSS)-induced colitis with spleen-kidney yang deficiency syndromes: role of gut microbiota, fecal metabolites, inflammatory dendritic cells, and TLR4/NF-κB pathway. *Evid Based Complement Alternat Med*. 2022;2022:6132289. doi:10.1155/2022/6132289
18. Zhang XY, Zhao HM, Liu Y, et al. Sishen Pill maintained colonic mucosal barrier integrity to treat ulcerative colitis via Rho/ROCK signaling pathway. *Evid Based Complement Alternat Med*. 2021;2021:5536679. doi:10.1155/2021/5536679
19. Chen F, Yin YT, Zhao HM, et al. Sishen Pill treatment of DSS-induced colitis via regulating interaction with inflammatory dendritic cells and gut microbiota. *Front Physiol*. 2020;11:801. doi:10.3389/fphys.2020.00801
20. Zhao T, Wang Z, Liu Z, Xu Y. Pivotal role of the interaction between herbal medicines and gut microbiota on disease treatment. *Curr Drug Targets*. 2021;22(3):336–346. doi:10.2174/1389450121666200324151530

21. Yang M, Hong G, Jin Y, Li Y, Li G, Hou X. Mucosal-associated microbiota other than luminal microbiota has a close relationship with diarrhea-predominant irritable bowel syndrome. *Front Cell Infect Microbiol*. 2020;10:515614. doi:10.3389/fcimb.2020.515614
22. Xie S, Fang L, Deng N, Shen J, Tan Z, Peng X. Targeting the gut-kidney axis in diarrhea with kidney-yang deficiency syndrome: the role of Sishen pills in regulating TMAO-mediated inflammatory response. *Med Sci Monit*. 2024;30:e944185. doi:10.12659/MSM.944185
23. Wu Y, Peng X, Li X, Li D, Tan Z, Yu R. Sex hormones influence the intestinal microbiota composition in mice. *Front Microbiol*. 2022;13:964847. doi:10.3389/fmicb.2022.964847
24. Li X, Qiao B, Wu Y, Deng N, Yuan J, Tan Z. Sishen pill inhibits intestinal inflammation in diarrhea mice via regulating kidney-intestinal bacteria-metabolic pathway. *Front Pharmacol*. 2024;15:1360589. doi:10.3389/fphar.2024.1360589
25. Qiao B, Liu J, Deng N, et al. Gut content microbiota dysbiosis and dysregulated lipid metabolism in diarrhea caused by high-fat diet in a fatigued state. *Food Funct*. 2023;14(8):3880–3892. doi:10.1039/D3FO00378G
26. Zhou M, Li X, Liu J, Wu Y, Tan Z, Deng N. Adenine's impact on mice's gut and kidney varies with the dosage administered and relates to intestinal microorganisms and enzyme activities. *3 Biotech*. 2024;14(3):88. doi:10.1007/s13205-024-03959-y
27. Heng X, Liu W, Chu W. Identification of choline-degrading bacteria from healthy human feces and used for screening of trimethylamine (TMA)-lyase inhibitors. *Microb Pathog*. 2021;152:104658. doi:10.1016/j.micpath.2020.104658
28. Ferrell M, Bazeley P, Wang Z, et al. Fecal microbiome composition does not predict diet-induced TMAO production in healthy adults. *J Am Heart Assoc*. 2021;10(21):e021934. doi:10.1161/JAHA.121.021934
29. Li X, Deng N, Zheng T, et al. Importance of Dendrobium officinale in improving the adverse effects of high-fat diet on mice associated with intestinal contents microbiota. *Front Nutr*. 2022;9:957334. doi:10.3389/fnut.2022.957334
30. Segata N, Izard J, Waldron L, et al. Metagenomic biomarker discovery and explanation. *Genome Biol*. 2011;12(6):R60. doi:10.1186/gb-2011-12-6-r60
31. Montoro-Dasi L, Lorenzo-Rebenaque L, Ramon-Moragues A, et al. Antibiotic removal does not affect cecal microbiota balance and productive parameters in LP robust rabbit line. *Front Vet Sci*. 2022;9:1038218. doi:10.3389/fvets.2022.1038218
32. Zhou W, Cheng Y, Zhu P, Nasser MI, Zhang X, Zhao M. Implication of gut microbiota in cardiovascular diseases. *Oxid Med Cell Longev*. 2020;2020:5394096.
33. Chávez-Carbajal A, Nirmalkar K, Pérez-Lizaur A, et al. Gut microbiota and predicted metabolic pathways in a sample of Mexican women affected by obesity and obesity plus metabolic syndrome. *Int J Mol Sci*. 2019;20(2):438. doi:10.3390/ijms20020438
34. Bui TVA, Hwangbo H, Lai Y, et al. The gut-heart axis: updated review for the roles of microbiome in cardiovascular health. *Korean Circ J*. 2023;53(8):499–518. doi:10.4070/kcj.2023.0048
35. Fernández-Olmos A, García-Castillo M, Morosini MI, Lamas A, Máiz L, Cantón R. MALDI-TOF MS improves routine identification of non-fermenting Gram negative isolates from cystic fibrosis patients. *J Cyst Fibros*. 2012;11(1):59–62. doi:10.1016/j.jcf.2011.09.001
36. Ruiz-Malagón AJ, Rodríguez-Sojo MJ, Hidalgo-García L, et al. The antioxidant activity of thymus serpyllum extract protects against the inflammatory state and modulates gut dysbiosis in diet-induced obesity in mice. *Antioxidants*. 2022;11(6):1073. doi:10.3390/antiox11061073
37. Shang Q, Song G, Zhang M, et al. Dietary fucoidan improves metabolic syndrome in association with increased *Akkermansia* population in the gut microbiota of high-fat diet-fed mice. *Journal of Functional Foods*. 2017;28:138–146. doi:10.1016/j.jff.2016.11.002
38. Mori G, Orena BS, Cultrera I, et al. Gut microbiota analysis in postoperative lynch syndrome patients. *Front Microbiol*. 2019;10:1746. doi:10.3389/fmicb.2019.01746
39. Zhu HZ, Liang YD, Ma QY, et al. Xiaoyaosan improves depressive-like behavior in rats with chronic immobilization stress through modulation of the gut microbiota. *Biomed Pharmacother*. 2019;112:108621. doi:10.1016/j.biopha.2019.108621
40. He Q, Zhang Y, Ma D, Zhang W, Zhang H. Lactobacillus casei Zhang exerts anti-obesity effect to obese glut1 and gut-specific-glut1 knockout mice via gut microbiota modulation mediated different metagenomic pathways. *Eur J Nutr*. 2022;61(4):2003–2014. doi:10.1007/s00394-021-02764-0
41. Ju T, Kong JY, Stothard P, Willing BP. Defining the role of Parasutterella, a previously uncharacterized member of the core gut microbiota. *ISME J*. 2019;13(6):1520–1534. doi:10.1038/s41396-019-0364-5
42. Gabr M, Świderek K. Discovery of a histidine-based scaffold as an inhibitor of gut microbial choline trimethylamine-lyase. *ChemMedChem*. 2020;15(23):2273–2279. doi:10.1002/cmdc.202000571
43. Cai YY, Huang FQ, Lao X, et al. Integrated metagenomics identifies a crucial role for trimethylamine-producing Lachnoclostridium in promoting atherosclerosis. *NPJ Biofilms Microbiomes*. 2022;8(1):11. doi:10.1038/s41522-022-00273-4
44. Zhu Y, Jameson E, Crosatti M, et al. Carnitine metabolism to trimethylamine by an unusual Rieske-type oxygenase from human microbiota. *Proc Natl Acad Sci U S A*. 2014;111(11):4268–4273. doi:10.1073/pnas.1316569111
45. Craciun S, Marks JA, Balskus EP. Characterization of choline trimethylamine-lyase expands the chemistry of glycyl radical enzymes. *ACS Chem Biol*. 2014;9(7):1408–1413. doi:10.1021/cb500113p
46. Lai Y, Tang H, Zhang X, et al. Trimethylamine-N-oxide aggravates kidney injury via activation of p38/MAPK signaling and upregulation of HuR. *Kidney Blood Press Res*. 2022;47(1):61–71. doi:10.1159/000519603
47. Ma G, Pan B, Chen Y, et al. Trimethylamine N-oxide in atherogenesis: impairing endothelial self-repair capacity and enhancing monocyte adhesion. *Biosci Rep*. 2017;37(2):BSR20160244. doi:10.1042/BSR20160244
48. Zhou X, Zhang B, Zhao X, et al. Chlorogenic acid prevents hyperuricemia nephropathy via regulating TMAO-related gut microbes and inhibiting the PI3K/AKT/mTOR pathway. *J Agric Food Chem*. 2022;70(33):10182–10193. doi:10.1021/acs.jafc.2c03099
49. Hou L, Tian HY, Wang L, et al. Identification and biosynthesis of pro-Inflammatory sulfonolipids from an opportunistic pathogen Chryseobacterium gleum. *ACS Chem Biol*. 2022;17(5):1197–1206. doi:10.1021/acschembio.2c00141
50. Craciun S, Balskus EP. Microbial conversion of choline to trimethylamine requires a glycyl radical enzyme. *Proc Natl Acad Sci U S A*. 2012;109(52):21307–21312. doi:10.1073/pnas.1215689109
51. Yoo W, Zieba JK, Foegeding NJ, et al. High-fat diet-induced colonocyte dysfunction escalates microbiota-derived trimethylamine N-oxide. *Science*. 2021;373(6556):813–818. doi:10.1126/science.aba3683
52. Seldin MM, Meng Y, Qi H, et al. Trimethylamine N-oxide promotes vascular inflammation through signaling of mitogen-activated protein kinase and nuclear factor-κB. *J Am Heart Assoc*. 2016;5(2):e002767. doi:10.1161/JAHA.115.002767

Journal of Inflammation Research Dovepress

Publish your work in this journal

The Journal of Inflammation Research is an international, peer-reviewed open-access journal that welcomes laboratory and clinical findings on the molecular basis, cell biology and pharmacology of inflammation including original research, reviews, symposium reports, hypothesis formation and commentaries on: acute/chronic inflammation; mediators of inflammation; cellular processes; molecular mechanisms; pharmacology and novel anti-inflammatory drugs; clinical conditions involving inflammation. The manuscript management system is completely online and includes a very quick and fair peer-review system. Visit http://www.dovepress.com/testimonials.php to read real quotes from published authors.

Submit your manuscript here: https://www.dovepress.com/journal-of-inflammation-research-journal